H13-74
3D STRATIFIED ATMOSPHERIC FLOW MODELING

Aleš Jirk[1] and Josef Brechler[1]

[1]Charles University, Faculty of Mathematics and Physics, Department of Meteorology and Environment Protection, V Holesovickach 2, 180 00 Prague, The Czech Republic

Abstract: This contribution considers the influence of stratification on incompressible flow for low values of Reynolds numbers. As a test problem, 3D cavity flow is modeled and the results compared with those published previously. The influence of stratification is also examined in the case of flow past an obstacle located inside a channel. The flow and intensity of stratification are characterized by the Reynolds number *Re* and the Froude number *Fr*, respectively. The Froude number, which determines the stability of the stratified flow (the ratio of buoyancy to the inertia force), is the inverse of the Richardson number *Ri*. For *Ri* of 0.1–10.0, both forces contribute to the flow structure, and the flow can be considered as mixed convection. The employed model consists of the Navier–Stokes equations with the Boussinesq approximation, the continuity equation in the form for incompressible fluid flow, and the prognostic equation for fluctuations in potential temperature. Conservative high-order methods are used to solve the system of equations. The advection terms are reconstructed using the fifth-order WENO scheme and temporal evolution is solved by application of the explicit TVD (total variation diminishing) Runge–Kutta scheme. Near the borders of the obstacle wall functions are employed. We also comment on the application of TVD and non-TVD Runge–Kutta temporal integration.

Key words: 3D stratified flow, WENO scheme, Runge–Kutta scheme.

INTRODUCTION

Any atmospheric flow within the atmospheric boundary layer is turbulent and almost non-neutrally stratified. In this contribution, we focus on the problem of laminar flow of stably stratified fluid. As a consequence of stratification, we are able to observe meteorological phenomena such as gravity waves and wake effects in regions located behind obstacles.

To prevent the occurrence of undesired spurious oscillations in our numerical modeling, we employed the finite volume approach with higher-order (fifth-order) WENO reconstruction. For temporal discretization, we employed the explicit TVD (Total Variation Diminishing) Runge–Kutta (R–K) scheme. We examined several types of TVD and non-TVD R–K schemes with different degrees of accuracy.

To test the applicability of this approach, we chose a problem involving flow in a cavity, around a square cylinder in a channel. The lid-driven cavity flow case was computed for several values of the Courant–Friedrichs–Lewy (CFL) condition. Stratification was considered in the computation using the prescribed gradient in potential temperature. In the case of cavity flow, the gradient was set via the prescribed temperatures at the top and bottom boundaries of the model domain. The lid-driven cavity flow problem was then computed in 2D and 3D. In the flow past an obstacle, we used a similar temperature gradient to that in the cavity. As the problem is solved in terms of non-dimensional variables, the temperature of the upper lid was maintained at a value of 1, and the temperature of the bottom lid was equal to zero.

The strength of stratification is characterized by a non-dimensional parameter - the Froude number *Fr*, which is the inverse of the Richardson number *Ri*. For positive values of *Ri* and $Ri \gg 1$, (negative) buoyancy force is dominant. The inertia force is equal to the buoyancy force for $Ri \approx 1$, whereas for $Ri \ll 1$ (but still positive) the inertia force dominates. For *Ri* in the range 0.1–10.0, both forces contribute to the flow structure, and the fluid motion can be considered as mixed convection (see Mohamad,A., A. and Viskanta, R. 1995).

GOVERNING SYSTEM

The governing equations that describe fluid motion are the Navier–Stokes equations (1) and the continuity relation (2). Stratification is employed using the Boussinesq approximation, which adds an equation for perturbations in potential temperature (3) to the system. All these equations (1–3) are in Jirk,A. 2008 and are written in a non-dimensional form:

$$\frac{\partial v_i}{\partial t} + \frac{\partial v_i v_k}{\partial x_k} = -\frac{\partial p\ll}{\partial x_i} + \frac{1}{\text{Re}}\Delta v_i + \frac{1}{Fr}\frac{\theta\ll}{\overline{\theta}}, \tag{1}$$

$$\frac{\partial v_i}{\partial x_i} = 0, \tag{2}$$

$$\frac{\partial \theta\ll}{\partial t} + v_k\frac{\partial \theta\ll}{\partial x_k} = -v_3\frac{\partial \overline{\theta}}{\partial x_i}, \tag{3}$$

where *i, k* = 1,3 for the 2D approach and *i, k* = 1,2,3 for the 3D approach, v_i are velocity components, θ' is perturbation in potential temperature, $\overline{\theta}$ is the average value of potential temperature, *p'* is pressure perturbation, x_i are coordinates, and *t* is time.

The following paragraph gives a short description of the set up for figures, equations and tables.

NUMERICAL METHODS

The finite volume method is used for spatial discretization of the governing equations (1–3) (e.g., Ferziger, J. H. and Perić, M. 1997 and McDonough, J.M. 2003). The advection terms in (1) and on the left-hand side of (3) are reconstructed using the WENO scheme (Liu et al. 1994), which is used to reconstruct the values of velocity components at the control volume (CV) boundaries, which are required to assess the magnitude of numerical fluxes. When reconstructing the velocity at the CV

boundaries, the WENO scheme uses all possible stencils (depending on the order of reconstruction) with corresponding weights. Weights are computed from the total variation for a given stencil. The highest weight is obtained for the stencil with the lowest total variation. Here, we employ the WENO scheme with fifth-order accuracy. Viscous terms in (1) were computed using the Crank–Nicholson method (Kim et al. 2001). For discretization of the temporal partial derivation in (1) and (3), we used the explicit TVD R–K scheme with fourth- and third-order accuracy (Strang, G. 1964). The fractional-step method (Brown et al. 2001) was employed to solve the Navier–Stokes equations (1) and continuity relation (2). This approach un-groups the solution of equations into several steps; here, we employ a two-step method. For simulation of the obstacle, we employed a direct forcing immersed boundary method (Kim et al. 2001) with second-order accuracy.

NUMERICAL EXPERIMENTS

As stated above, several types of TVD and non-TVD R–K schemes were tested on Euler equations. We compared the third- and fourth-order TVD schemes with the fourth-order non-TVD R–K scheme.

a

b
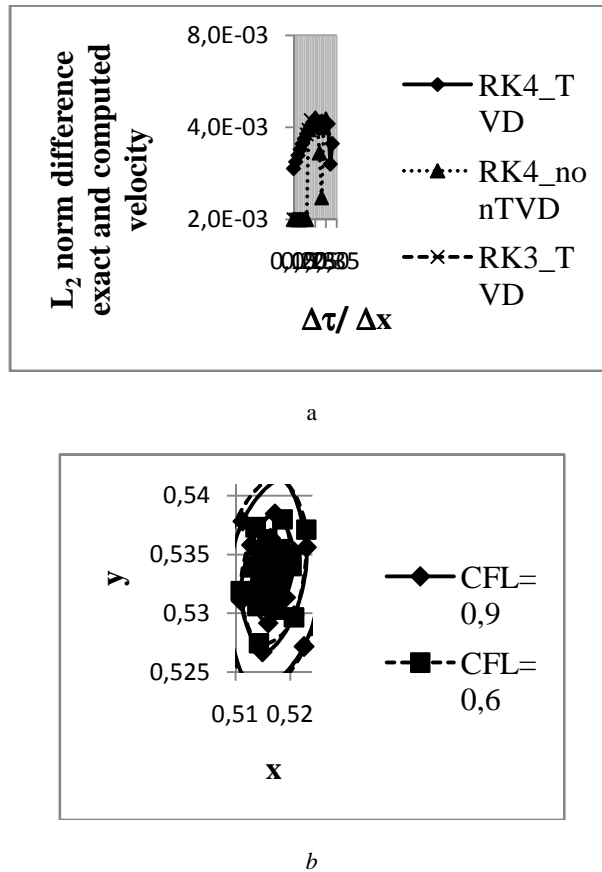
Figure 1. Stability testing of the Runge–Kutta scheme: a) Euler equation for a grid size of 129^2, b) Navier–Stokes equation

All these schemes are described in Shu,Ch.W. and Osher, S. 1988. The R–K schemes were tested for three grid sizes: 129^2, 193^2, and 257^2. The dependence of L_2 norm on the ratio $\Delta\tau/\Delta x$ for various types of R–K schemes (figure 1a) reveals that the fourth-order TVD R–K scheme is the most stable among the three schemes and that the TVD schemes have smoother courses than do the non-TVD schemes. The results are similar for all three grid sizes.

Figure 1b shows the results of a stability test for the lid-driven cavity case; i.e., a test of the stability of the Navier–Stokes equations. The temporal convergence of the primary vortex center to its stable position is shown for two different values of the coefficient $\Delta\tau/\Delta x$. The convergence is more accurate and faster for the coefficient with a lower value.

FORMULATION OF THE PROBLEM

We simulated and compared three cases of stratified flow. The first and second cases deal with 2D and 3D lid-driven cavity flow influenced by stratification. The 2D flow pattern with neutral stratification is compared with the results of Ghia *et al.* 1982, and the results obtained with stratified flow are compared with those of Iwatsu *et al.* 1992 and Iwatsu,R. and Hyun,J.M. 1995. The boundary conditions are Dirichlet conditions for the components of velocity and average potential temperature: $v = 0$ ($w = 0$ for the 3D case) at all boundaries, $u = 0$ at the side and bottom boundaries, $u = 1$ at the top boundary, $\bar{\theta} = 0$ at the bottom boundary, and $\bar{\theta} = 1$ at the top boundary. For perturbations in potential temperature, we use a linear extrapolation to the boundaries. The third case deals with 2D stratified flow past a square cylinder located in a channel, using the following conditions: for channel inflow, a Dirichlet condition $v = 0$ is used together with a parabolic profile of the u component (with $u = 1$ in the parabola centre); the magnitude is reduced to zero toward the boundaries. At the outflow,

Neumann conditions $\frac{\partial u}{\partial x} = \frac{\partial v}{\partial x} = 0$ are used. For perturbations in potential temperature, linear extrapolation is applied to the boundaries. The Reynolds number is 200 and the Froude numbers are 1.00, 0.10, and 0.01, respectively.

RESULTS, DISCUSSION

Here, we present some of the results of 2D and 3D computations of stratified lid-driven cavity flow. Figure 2a shows 2D cavity flow for $Re = 100$ and $Fr = 0.1$. Figure 2b shows the case for 3D (showing a cross-section located mid-cavity, $y = 0.5$) and for $Re = 400$. And in figure 3 is depicted distribution of perturbation of potential temperature of cavity for Re = 400. The strength of stable stratification means that the primary vortex is largely confined to the upper part of the cavity. The influence of the upper boundary velocity (primary vortex) extends over a smaller area within the cavity because the stable stratification acts to suppress vertical motion. Vertical exchange is strongly suppressed, especially in the lower part where it becomes chaotic.
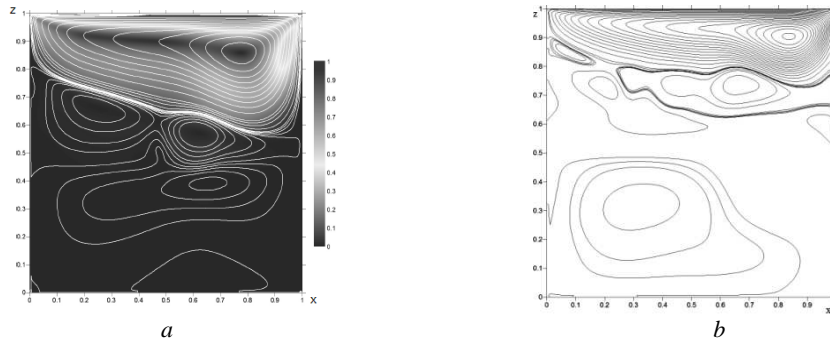
Figure 2. Streamlines of the flow field for $Fr = 0.1$: a) 2D, velocity magnitude, $Re = 100$
b) cross-section through the 3D simulation, $Re = 400$
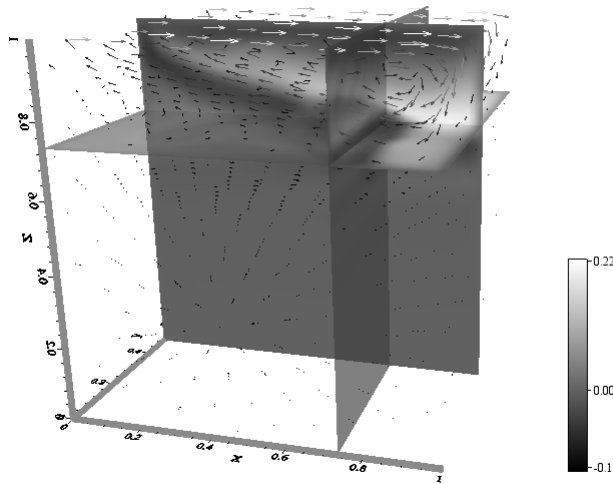
Figure 3. Field of potential temperature, arrows of flow field cross-section through the 3D simulation (planes x=0.75, y=0.5, z=0.75),
$Re = 400$, Fr = 0.1

The results shown in Figure 2a, 2b and 3 are qualitatively consistent with the results of Iwatsu *et al.* 1992, Iwatsu,R. and Hyun,J.M. 1995, and Tae *et al.* 2007.
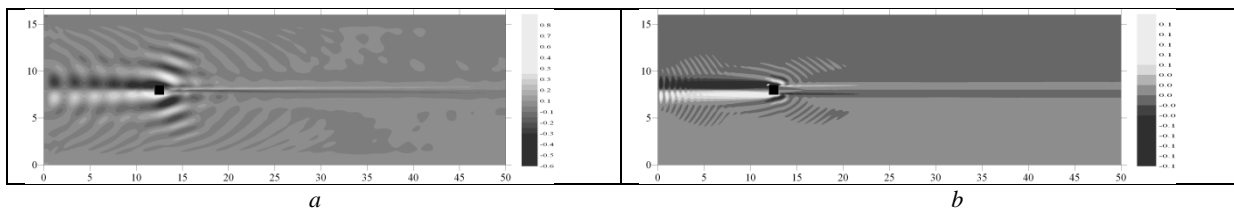
Figure 4. Field of potential temperature perturbations for: a) Fr = 0.1, b) Fr = 0.01

Figure 4a and 4b shows the results of stratified 2D flow past a square cylinder; the fields of potential temperature perturbations are shown for $Fr = 0.1$ (less stable) and 0.01 (more stable). The results support the assumption that with decreasing Fr, the wake effects behind the obstacle are less pronounced, as the gravitational waves induced by the obstacle are more intensive and are emanated with a higher frequency. The results are also consistent with the known situation in the atmosphere and the value of the well-known Brunt–Väisälä frequency. A higher value of Brunt–Väisälä frequency is obtained with more stably stratified fluid. This relationship is confirmed when the dependence of velocity on time is computed. With decreasing Fr, velocity oscillations are generated by the obstacle (see (4)) at higher frequencies:

$$f(Fr = 0.01) = 1.63, \quad f(Fr = 0.10) = 0.79, \quad f(Fr = 1.00) = 0.30 \tag{4}$$

For flow around a square cylinder without the influence of stratification, the Strouhal number is $St \approx 0.13 - 0.14$ (Jirk, A. 2008). As Fr approaches ∞, the frequency of velocity approaches the Strouhal number.

CONCLUSIONS

We employed a fifth-order WENO reconstruction of the convective terms of Navier–Stokes equations and a Boussinesq approximation to describe the influence of stratification on laminar and incompressible flow. The results were compared with those of previous studies. As test examples, we considered stratified flow in a cavity and around an obstacle. The effect of stratification (assessed in terms of Fr) was in accordance with the known situation in stably stratified atmospheric flows. When Fr is large, the influence of stratification is weak (close to a neutrally stratified atmosphere). With decreasing Fr, the wake effects behind the obstacle become less pronounced and gravitational waves are induced more intensively and with higher frequencies due to the increasing stabilizing influence of stratification. In the case of cavity flow, circulation is largely confined to the upper region of the cavity and vertical motion is suppressed. The present results deal with 2D and 3D modeling.

ACKNOWLEDGMENTS

REFERENCES
Brown, D. L., Cortez, R. and Minion, L. M., 2001: Accurate Projection Methods for the Incompressible Navier-Stokes Equations. Journal of Computational Physics 168, 464-499.

Ferziger, J. H. and Peric, M., 1997: Computational Methods for Fluid Dynamics. Springer Verlag, Berlin.

Ghia, U., Ghia, K. N. and Shin, C. T., 1982: High-Resolutions for Incompressible Flow Using the Navier-Stokes Equations and a Multigrid Metod. Journal of Computational Physics 48, 387-411.

Iwatsu, R. and Hyun, J., M., 1995: Three-dimensional driven-cavity flows with a vertical temperature gradient. Int. Journal Heat Mass Transfer. Vol 38, No.18.

Iwatsu, R., Hyun, J., M. and Kuwahara, K., 1992: Mixed convection in a driven cavity with a stable vertical temperature gradient. Int. Journal Heat Mass Transfer. Vol 36, No.6.

Jirk, A., 2008: Thermally stratified atmospheric flow modelling. Diploma thesis. Dept of Meteorology and Env. Protect., MFF UK Prague (in Czech).

Kim, J., Kim, D. and Choi, H., 2001: An Immersed-Boundary Finite-Volume Method for Simulations of Flow in Complex Geometry. Journal of Computational Physics 171, 132-150.

Liu, X. D., Osher, S. and Chan T., 1994: Weighted Essentially Non-Oscillatory Schemes. Journal of Computational Physics 115, 200-212.

McDonough, J. M., 2003: Lectures in Computational Fluid Dynamics of Incompressible Flow: Mathematics, Algorithms and Implementations. Departments of Mechanical Engineering and Mathematics University of Kentucky.

Mohamad, A., A. and Viskanta, R., 1995: Flow and heat transfer in a lid-driven cavity filled with a stably stratified fluid. Applied Mathematical Modelling, vol. 19.

Shu,Ch.W. and Osher,S., 1988: Efficient Implementation of Essentially Non-Oscillatory Shock-Capturing Schemes,II. Journal of Computational Physics 83,32-78

Strang, G., 1964: Accurate Partial Difference Methods, II. Non-Linear Problems. Numerische Matematik 6, 37-46.

Tae, H. J., Seo, Y., K., Jie, M., H., 2007: Transient mixed convection in an enclosure driven by a sliding lid. Heat Mass Transfer 43, 629-638.